geosciences

MDPI

Article

The Sacred Waterscape of the Temple of Bastet at Ancient Bubastis, Nile Delta (Egypt)

Julia Meister [1,*], Philipp Garbe [1], Julian Trappe [1], Tobias Ullmann [1], Ashraf Es-Senussi [2], Roland Baumhauer [1], Eva Lange-Athinodorou [3] and Amr Abd El-Raouf [4,5,*]

1 Physical Geography, Institute of Geography and Geology, Julius Maximilian University of Würzburg, 97074 Würzburg, Germany; philipp.garbe@stud-mail.uni-wuerzburg.de (P.G.); julian.trappe@uni-wuerzburg.de (J.T.); tobias.ullmann@uni-wuerzburg.de (T.U.); baumhauer@uni-wuerzburg.de (R.B.)
2 Ministry of Tourism and Antiquities of Egypt, Cairo 11534, Egypt; ashrafsenussi@yahoo.com
3 Egyptology, Institute for Ancient Studies, Julius Maximilian University of Würzburg, 97070 Würzburg, Germany; eva.lange@uni-wuerzburg.de
4 Geology Department, Faculty of Science, Zagazig University, Zagazig 44519, Egypt
5 School of Earth Sciences, Zhejiang University, Hangzhou 310027, China
* Correspondence: julia.meister@uni-wuerzburg.de (J.M.); ammohammed@science.zu.edu.eg (A.A.E.-R.)

Abstract: Sacred water canals or lakes, which provided water for all kinds of purification rites and other activities, were very specific and important features of temples in ancient Egypt. In addition to the longer-known textual record, preliminary geoarchaeological surveys have recently provided evidence of a sacred canal at the Temple of Bastet at Bubastis. In order to further explore the location, shape, and course of this canal and to find evidence of the existence of a second waterway, also described by Herodotus, 34 drillings and five 2D geoelectrical measurements were carried out in 2019 and 2020 near the temple. The drillings and 2D ERT surveying revealed loamy to clayey deposits with a thickness of up to five meters, most likely deposited in a very low energy fluvial system (i.e., a canal), allowing the reconstruction of two separate sacred canals both north and south of the Temple of Bastet. In addition to the course of the canals, the width of about 30 m fits Herodotus' description of the sacred waterways. The presence of numerous artefacts proved the anthropogenic use of the ancient canals, which were presumably connected to the Nile via a tributary or canal located west or northwest of Bubastis.

Keywords: ancient Egypt; Tell Basta; *Isheru*; sacred lakes; Herodotus; ERT; drilling

Citation: Meister, J.; Garbe, P.; Trappe, J.; Ullmann, T.; Es-Senussi, A.; Baumhauer, R.; Lange-Athinodorou, E.; El-Raouf, A.A. The Sacred Waterscape of the Temple of Bastet at Ancient Bubastis, Nile Delta (Egypt). *Geosciences* **2021**, *11*, 385. https://doi.org/10.3390/geosciences11090385

Academic Editors: Peter Fischer, Tina Wunderlich and Jesus Martinez-Frias

Received: 14 August 2021
Accepted: 8 September 2021
Published: 10 September 2021

1. Introduction

Ancient Egyptian temples were essential elements of cities and settlements and were of great economic, administrative, religious, and cultic importance. The development of a city in ancient Egypt was therefore always linked to the presence of the temples of one or more local deities [1]. The temple areas (i.e., the temenos), thought to be the residences of deities, were most sacred and were characterized by the use of specific architecture and a multitude of other elements that emphasized their importance and enabled daily cultic and other activities [2,3].

Sacred water canals or lakes, the so-called *Isheru* of the ancient Egyptian texts, were distinctive constituting features of such temples. These sacred water bodies provided water for all kinds of purification rites and activities. Most central, however, was their role in the performance of the core element of many religious temple festivals, the rowing of the sacred barque of the deity. The *Isheru* were especially associated with temples of goddesses who appeared as lionesses, for instance as Sekhmet, Mut, Wadjet, and Bastet. Because the lion goddesses were of an ambivalent nature, oftentimes considered mighty and fierce, the presence of a cooling water body close to their temples was supposed to calm their fiery

temperaments as well as to protect the cities' inhabitants from their potential rage [3–6]. In the Nile Valley such *Isheru* were found, for example, in Thebes, Luxor, and Memphis [5,7,8].

In Egyptology, knowledge of the existence of sacred lakes or canals connected to temple buildings in the Nile Delta mainly depends on religious texts. Textual sources indicate the existence of such sacred watery landscapes at Buto [4] and Sais [4,9,10] in the western delta, Busiris in the central delta [4], and Tanis [11,12] and Bubastis [2] in the eastern delta (Figure 1a).

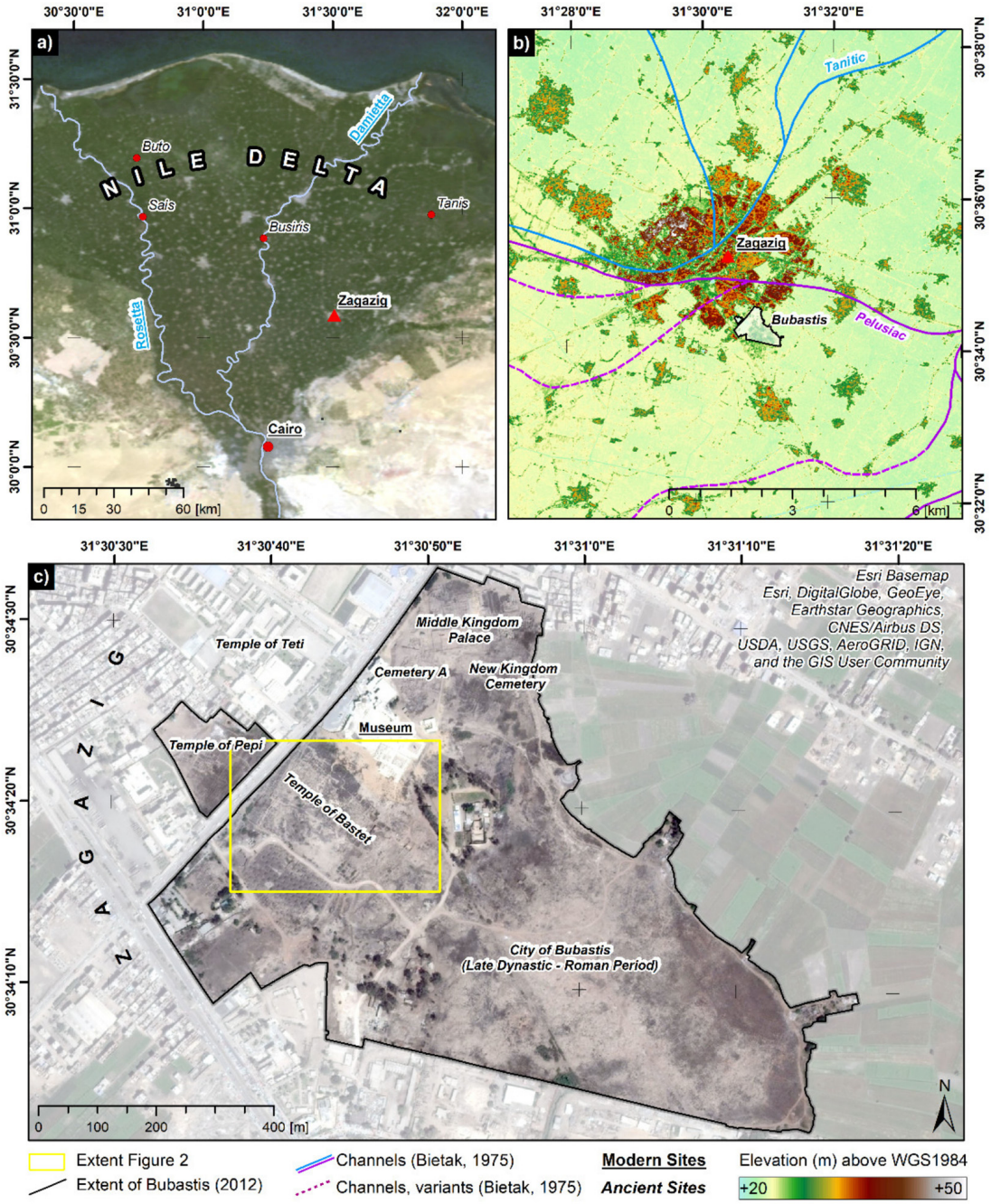

Figure 1. (**a**) Location of the modern town Zagazig in the Nile Delta, Egypt (Database: Terra MODIS True Color Corrected Reflectance from August 2020, © earthdata.nasa.gov); (**b**) Location and extent of ancient Bubastis in Zagazig (Database: Digital Elevation model of the TanDEM-X Mission, ©DLR, 2012); (**c**) Current extent of Bubastis with ancient and modern features (Database: © Esri Basemap).

Recently, new evidence has become available. Preliminary sedimentological analyses of core drillings and geophysical surveys provide valuable geoarchaeological evidence, allowing deeper investigations of the location, shape, and course of sacred water bodies at the temple sites of Buto, Sais, and Bubastis [3]. However, a truly comprehensive, multi-methodological approach to reconstructing the sacred landscape of a deltaic temple could only be applied to the archaeological site of Bubastis [2,13], where the existence of a canal in the northeast of the Temple of Bastet has been documented for the first time outside ancient writings [2].

This study continues the preliminary investigations and presents the results of combined 2D electrical resistivity tomography (ERT) and geomorphological surveying (i.e., drilling and sediment analyses) conducted in 2019 and 2020. The aim of the current investigations is to further explore the location, shape, and course of the already detected northern canal and to provide evidence on the existence of a second canal described by Herodotus in the 5th century BCE. In the past, 2D Electrical Resistivity Tomography (ERT) was commonly applied to delineate sedimentological differences of the subsurface without soil disturbance (e.g., [14–18]). In particular, the combination of geoelectrical resistivity mapping (i.e., vertical electrical soundings, ERT) and drilling has been applied successfully in the Nile Delta and Nile Valley in related studies aiming to identify and localize buried channels (e.g., [19–23]).

2. Study Area

2.1. Holocene Nile Delta Evolution and Settlement Activities

The Nile Delta is an alluvial plain formed from the Eocene up to the Middle Holocene by a long series of deltaic formations and controlled by natural factors such as tectonics and climate and sea level fluctuations [24–26]. The geological evolution of the Nile Delta is quite complex and shows regional differences, especially between the western and eastern delta [27]. From the Pleistocene onwards, it was characterized by alluvial accumulations of the *Mit Ghamr Formation* (Pre-Nile sediments) as well as the *Bilqas Formation* (Neo-Nile sediments). The *Mit Ghamr Formation* consists of numerous smaller units with various genetic origins of Pleistocene age deposited during a previous, interlocked Nile regime. Up to about 8000 cal BP, this material was eroded or translocated by the ancient Nile branches. Fluvial sands at local hills, often redeposited by aeolian processes, formed the *Geziracover Formation*, widely known as "turtlebacks" or *geziras* [28]. As a result of the Middle Holocene African humid period, hydrological variations and enhanced sediment supply led to high accumulation rates in the Nile Delta. Consequently, the bluish-black, organic-rich, silty-clayey to clayey-silty deposits of the *Bilqas-2 Formation* and brownish-greyish sediments with lower organic contents of the *Bilqas-1 Formation* overlayed the *geziras* [28–31].

Ancient settlement activity in the Nile Delta was strongly influenced by the Holocene delta evolution. Today, there are only two estuaries in the Nile Delta (the Rosetta and Damietta branches), although for antiquity up to seven large river branches are described in text sources, which have since silted up or been canalized. Due to their great importance for regional and supra-regional traffic and trade, as well as for the availability of water, major ancient Egyptian settlements were only found in the immediate vicinity of large Nile branches. In addition, if not established on the sandy elevations of the *geziras* or other geomorphological features, settlements were often built on the riverbanks, as protection against the Nile floods [32,33].

Overall, *geziras* and the various river branches were the dominant landscape features of the delta plain. Additionally, temples and cemeteries in the delta were usually built on top of natural elevations [34], such as *geziras* [26,35]. Therefore, sacred landscapes in the delta were usually characterized by an elevated temple connected to a body of water, whether in the form of a river, canal, lake, or pond [3].

2.2. The Ancient City of Bubastis (Tell Basta)

The ancient town of Bubastis ranked amongst the most important cities of the Nile Delta from the beginning of its occupation at around the transitional time from the 4th to the 3rd millennium BCE until the end of the Ptolemaic Period in 30 BCE. The excavation site of Bubastis (Tell Basta) is located in the southeastern Nile Delta at the southeastern city border of Zagazig (30° 57′ N, 31° 51′ E; 8 m a.s.l.), the capital of the Egyptian province of Sharqiya (Figure 1). Ancient Bubastis had access to the Pelusiac and perhaps also the Tanitic branch of the Nile, although the exact course and chronology of these Nile arms have not yet been determined (cf. [36–38]; Figure 1b). The additional vicinity of the Wadi Tumilat, the traditional overland route to Sinai and Palestine, gave Bubastis a very advantageous geographical position. In early times, the city held an important position within a trans-regional trade network that included the Levant and the southern Nile Valley. These attractive geographical conditions not only led to the initial development of the city, which probably began in the Predynastic period (c. 3200 BCE) but seem to have been an important factor in the city's continued importance until its gradual decline during the Roman period (ca. 200 CE). Another reason for the important role of Bubastis was its function as the main cult center of Bastet, the local feline deity, whose temple gained significance especially towards the end of the Old Kingdom (from the beginning of the 6th dynasty, at around 2300 BCE; [39]). At the same time, Bubastis was the residence of high provincial officials [40], a development that might have started more than two centuries earlier, as the discovery of a provincial residence from the middle of the 4th dynasty reveals [41]. A governor's palace and an associated cemetery of the 12th dynasty (around 1830 BCE) indicate that Bubastis also had the status of a ruling regional center in the subsequent period of the Middle Kingdom [42–44]. The city reached its peak of importance as a residence city of the 22th dynasty of Libyan kings (c. 900–800 BCE), which was accompanied by the renovation and probable enlargement of the local main deity Bastet and her temple [45–48].

The temple of the local deity Bastet is located on the central elevation of the underlying *gezira* ([13]; Figure 1c). Only a fraction of the original stone material remains visible on the surface. Its poor condition and the loss of a large part of the architecture complicates the reconstruction of the ground plan. However, the general arrangement of the columned courtyards and halls at the time of the Libyan 22nd Dynasty (under Kings Osorkon I and Osorkon II c. 924–850 BCE) can be identified [48–50].

The sacred waters of the Temple of Bastet appear prominently in the written record. An important source is the so-called Delta papyrus (Papyrus Brooklyn 47.218.84) from the second half of the 7th century BCE, which contains mythological tales of cities of the Nile Delta. The chapter about Bubastis describes the statue of Bastet in the temple as follows: "[. . .] An *Henet*-water of the water surrounds her completely. [. . .]", with the ancient Egyptian term *Henet* referring to natural water bodies [3,44,51]. The same papyrus contains a description about the ritual of the rowing of her sacred barque: "And they row her (. . .) on the Isheru [. . .]" [3,44,51]. Additionally, an inscription on the eastern wall of the Ptolemaic enclosure of the Temple of Horus at Edfu can be interpreted as a description of the canals: "Bastet, the Great One, lady of Bubastis [. . .] under (whose temple) the Nile flows" [3,44].

Besides these mythological and therefore rather vague pictures, Herodotus' description from the 5th century BCE of the Temple of Bastet offers a more detailed characterization of the temple's surroundings: "[...] Except the entrance, the rest is an island. The canals, which come from the Nile, are not joining one another, but each one extends to the entrance of the temple; the one surrounds the one side, the other the other side and each one is 100 feet wide and shadowed by trees [...]" [3,52].

To investigate the sacred landscape of the Temple of Bastet, a remote sensing-based study was recently conducted [53], which was supplemented by initial sedimentological and geophysical investigations [2,13]. Drilling and sediment analyses revealed clayey/silty deposits of several meters in thickness in the north of the Temple of Bastet, which itself is

grounded on Pleistocene *gezira* sands [13]. The recovered sediments were situated below the floor level (3.35 m a.s.l.) of the Temple of Bastet of the 1st mill. BCE and contained numerous anthropogenic artefacts. Direct current resistivity (DCR) sounding and 2D ERT surveying were conducted and confirmed the drilling results, with low resistivity values indicating trench-like layers. The recovered deposits were interpreted as infills of a very low energy fluvial system, providing geoarchaeological evidence of a sacred canal north of the Temple of Bastet. Presumably, this waterway was connected to a branch of the Nile and has been silted up over time. Dating the canal and its active period was not possible [2], however, the textual sources indicate that the water system existed at least in the period from the 7th to the 5th century BCE [3].

3. Materials and Methods

Further geophysical and geomorphological investigations on the sacred canals continued in 2019 and 2020 with special emphasis on the verification of the second canal described by Herodotus (cf. above). For this purpose, on-site drilling and ERT surveying was extended in the vicinity north and south of the Temple of Bastet (Figures 1 and 2).

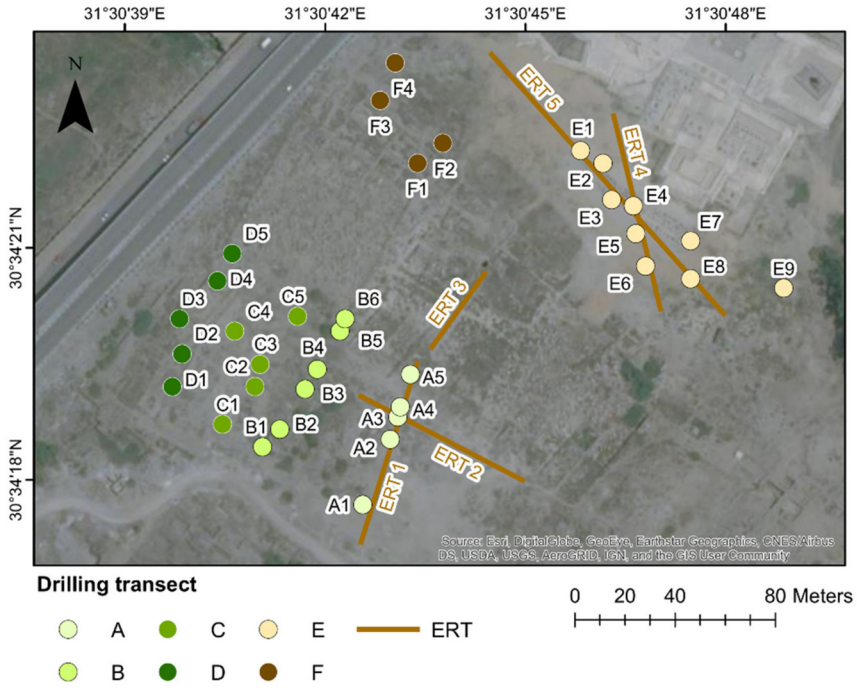

Figure 2. Overview of drilling locations and the position of 2D Electrical Resistivity Tomography (ERT) profiles (Database: © Esri Basemap).

3.1. Drillings and Sediment Analyses

The hand drillings of 2016 and 2018 [2,13] were supplemented by 34 percussion drillings in 2019 and 2020 using a vibracorer (Wacker BH 65, Wacker Neuson, Munich, Germany) with open steel auger heads of 8, 6, and 5 cm diameter and 1 m length. Drillings were carried out until the Pleistocene *gezira* sands were hit, reaching a maximum depth of 10.5 m. The drillings were arranged in transects in order to optimally match the possible courses of the canals (Figure 2), with four transects (A–D) in the south and two transects (E–F) in the north of the Temple of Bastet. The altitude given in m a.s.l. is based on a local reference system, established by the archaeological mission of Bubastis [2], and was measured by using an optical levelling instrument (Leica TS06, Leica Camera, Wetzlar, Germany). The ancient floor level of the Temple of Bastet is located at 3.35 m a.s.l. The drilling locations were documented using a standard GPS device (Garmin GPSMAP 60CSx, Lenexa, KS, USA). Retrieved sediments were lithologically described and analyzed on site, following KA5 [54] and FAO [55]. The grain sizes, texture, sediment color, the presence of

redoximorphic features, and special findings (ceramic fragments, charcoal, plant remains, bones, limestone, etc.) were documented. Since sample transport is restricted, no further laboratory analyses have been performed to date. However, archaeological artefacts (i.e., well-preserved ceramic fragments embedded in the sediment cores) serve as indicators for the chronostratigraphy.

3.2. Electrical Resistivity Tomography (ERT)

The information of the coring was compared to, and extended with, 2D ERT measurements in 2019 to derive a reconstruction of the former canal system. ERT surveying was conducted for five profiles (ERT 1–5) in locations based on the results of the drillings (Figure 2). The profiles ERT 1–2 are placed south of the Temple of Bastet and the profiles ERT 4–5 are located to its north. The profile ERT 3 is positioned in the center of the temple. The 2D ERT data was acquired using a IRIS Syscal R2 instrument. The Wenner-Beta (WB) configuration was used to estimate the apparent resistivity of the underlying sediments. The WB configuration is characterized by a high signal-to-noise ratio [56] and is commonly applied in geoarchaeological research [57]. It usually provides sufficient vertical resolution to accurately determine the structure of the subsurface and thus the location of expected canals or buried *gezira* sands. The ERT measurements were performed with two- or four-meter electrode spacing reaching lengths between 38 and 136 m (Table 1). The different electrode spacings were selected according to the results deduced from the drillings and caused different penetration depths and resolutions. The differences in terrain surface elevation were noted manually, even though their influence on the measurements is expected to be of minor relevance as the terrain is rather flat.

Table 1. Name, length, electrode spacing, and drilling locations of 2D ERT profiles.

Profile	Length [m]	Electrode Spacing [m]	Drilling Locations
ERT 1	76	2	A1–A5
ERT 2	76	2	A3
ERT 3	38	2	n.a.
ERT 4	84	2	E4–E6
ERT 5	136	4	E1–E4, E8

The 2D ERT profiles were processed and inverted using the software RES2DINV x64 ver. 4.08 [56]. This program is based on the smoothness-constrained least-squares inversion algorithm and was developed to produce a quick inversion process for 2D ERT measurements [58]. Five iterations were used to generate the 2D profiles. The Root Mean Square Error (RMS) was between 1.9% and 5.2%.

4. Results

4.1. Distribution of Sedimentary Units

In-field sedimentological analyses based on the investigation of all 34 drillings allowed three major lithological units to be distinguished due to their potential depositional milieu (*units I–III*; exemplarily illustrated for core E7 in Figure 3); another lithological unit (*unit IV*) was observed very sporadically. The simplified core stratigraphies are displayed together with the locations of the core sites in Figures 4 and 5 (see Table S1 for detailed core descriptions). The different lithological units are described and interpreted as follows:

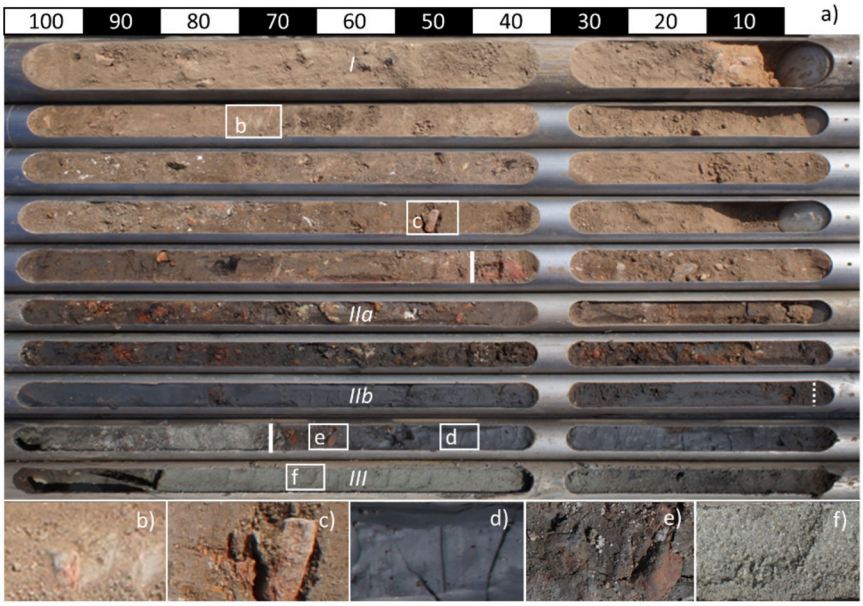

Figure 3. (**a**) Core stratigraphy of E7 showing the three major lithologic units: anthropogenic surface layer (*unit I*), clayey fluvial/limnic sediments with a high content of cultural debris (*unit II*a), clayey fluvial/limnic sediments with a low content of cultural debris (*unit II*b), and sands of fluvial origin (*unit III*). (**b**,**c**) Pottery fragments; (**d**) Clayey fluvial/limnic sediments; (**e**) Pottery fragments from a period before the 25th dynasty (i.e., before c. 728 BCE); (**f**) Sands of fluvial origin. Photos: J. Trappe 2019.

Unit I: All profiles are covered by an anthropogenic debris layer up to ~6 m thick, characterized by varying contents of modern and ancient debris such as ceramic, charcoal, brick, and limestone fragments. The texture is usually dominated by silt or sand; however, variable grain size distributions occur. The sediment colors range from light brownish to greyish, depending on the kind and number of artefacts.

Unit II: In many cores the anthropogenic surface layer is followed by loamy to clayey deposits which are characterized by dark brownish to greyish colors and higher soil moistures. These fine-grained deposits generally contain varying concentrations of anthropogenic debris, with a noticeable concentration at the bottom of the layer in some cores. Unfortunately, only a few pottery fragments were large enough to be dated. Their small grain sizes and dark coloring suggest a high organic content and indicate a fluvial or limnic depositional milieu, with a relatively low flow velocity. While these sediments are missing in some cores, their thickness varies considerably within the remaining cores, ranging from a few centimeters to about five meters.

Unit III: At the bottom of all cores, medium to coarse sandy deposits with varying gravel content occur, which are probably of fluvial origin, usually contain no anthropogenic debris and are yellowish to greyish-blue in color depending on the groundwater level.

Unit IV: Thin layers of yellowish, well-sorted fine to medium sands are found sporadically (i.e., A3, A4, B3). These deposits do not contain anthropogenic debris and are most likely of aeolian origin.

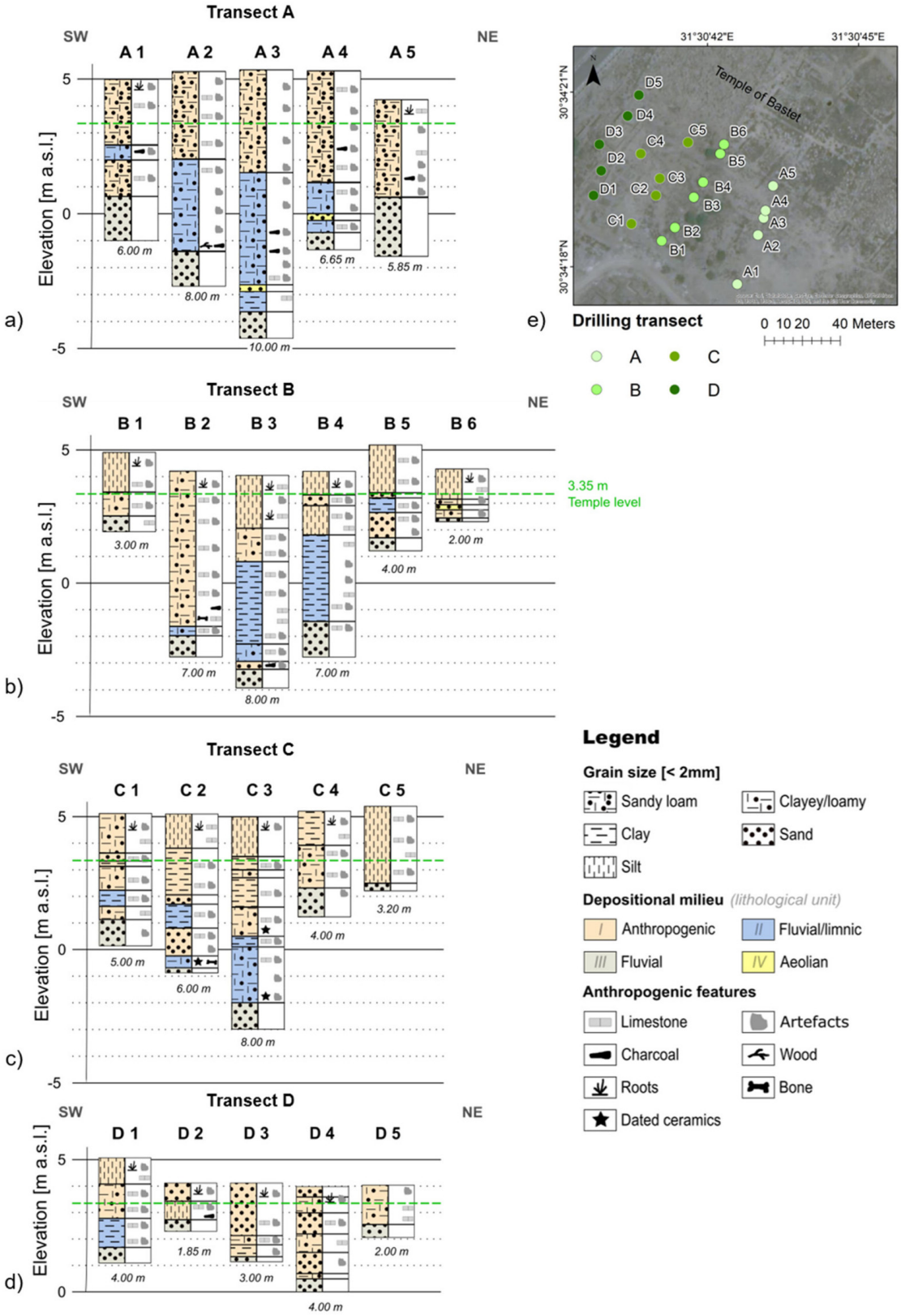

Figure 4. Drilling locations (**e**) and generalized results of drilling transects A–D in the south of the Temple of Bastet (**a**–**d**). The dashed green line marks the floor level of the Temple of Bastet in the 1st millennium BCE (3.35 m a.s.l.).

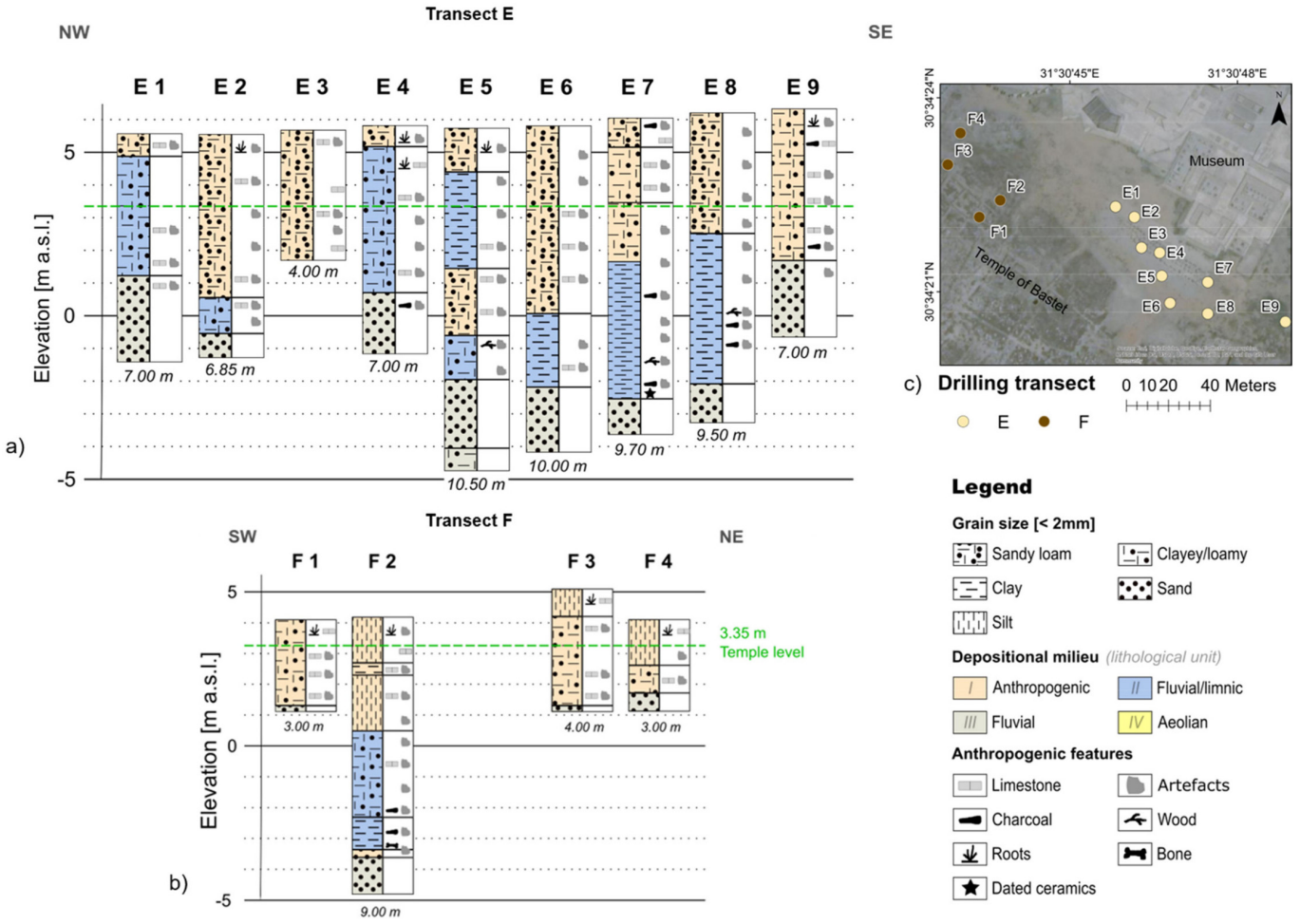

Figure 5. Drilling locations (**c**) and generalized results of drilling transects E–F in the north of the Temple of Bastet (**a**,**b**). The dashed green line marks the floor level of the Temple of Bastet in the 1st millennium BCE (3.35 m a.s.l.).

4.1.1. South of the Temple of Bastet (Drilling Transects A–D)

In the southwest of the temple, most cores contain loamy to clayey sediments of fluvial/limnic origin (*unit II*) below the anthropogenic layer (*unit I*), especially in the eastern part (Figure 4a–d). The basal layer of all cores consists of sand deposits of fluvial origin (*unit III*).

In transect A, the fine-grained sediments of *unit II* were detected in cores A1–A4 between 2.5 m and −3.5 m a.s.l. in various thicknesses (Figure 4a). While the thickness of these sediments in core A1 is relatively low at 0.6 m, cores A2–A4 show significantly thicker layers, ranging from 1.9 m to 5.2 m. Such fine-grained deposits are absent from core A5 and the anthropogenic debris layer (*unit I*) lies on top of the fluvial sands (*unit III*). The distribution of the fluvial/limnic sediments (*unit II*) within the transect shows a basin-like shape with a maximum thickness and depth of this layer in core A3.

Further northwest, transect B shows a comparable picture. Thick layers of clayey sediments of fluvial/limnic origin (*unit II*) are detectable between 3 m and −3 m a.s.l. with maximum thicknesses of 3.3 m to 3.8 m in the middle transect area of cores B4 and B3 (Figure 4b). Towards the southern and northern margins of the transect, the size of these clay-rich layers decreases to a few decimeters in cores B2 and B5. At the transect edges, in cores B1 and B6, such deposits are completely absent, and the anthropogenic debris layer (*unit I*) overlies fluvial sands (*unit III*).

Transect C shows loamy to clayey deposits of fluvial/limnic origin (*unit II*) towards the southwest (cores C1–C3), while the fluvial sands (*unit III*) in the northeastern transect area are only overlain by anthropogenic debris layers (cores C4–C5; Figure 4c). The fine-grained sediments of *unit II* occur at depths between 2 and −2 m a.s.l. and are much thinner than in transects A and B, ranging from 0.6 m to 2.5 m in cores C1–C3. In core C2, an anthropogenic debris layer (*unit I*) separates two layers of fluvial/limnic deposits (*unit II*). Ceramic fragments at the bottom of *unit II* in cores C2 and C3 can be assigned to the Old and Middle Kingdom (i.e., from c. 2700–1700 BCE).

In transect D, only core D1 in the southwestern transect part contains fine-grained deposits of *unit II* with 1.1 m thickness (i.e., situated between 2.8 and 1.8 m a.s.l.). In the cores D2–D5 towards the northeast, the anthropogenic layer (*unit I*) overlies the fluvial sands (*unit III*; Figure 4d).

Aeolian reworked sands of *unit IV*, each a few decimeters thick, were detected in cores A3, A4 and B6 at different depths (Figure 4a,b). In other cores, they were observed sporadically in very thin layers a few centimeters thick (cf. Table S1).

4.1.2. North of the Temple of Bastet (Drilling Transects E–F)

The drillings north of the Temple of Bastet show parallels to the drillings in the south (Figure 5). Again, most of the cores contain fluvial/limnic sediments (*unit II*) beneath the anthropogenic surface layer (*unit I*), especially to the east (transect E; Figure 5a,b). The bottom layers of the profiles consist of fluvial sands (*unit III*). Aeolian reworked sands of *unit IV*, on the other hand, were only observed in very thin layers of a few centimeters (cf. Table S1).

In transect E, loamy to clayey sediments of fluvial/limnic origin (*unit II*) were detected below the anthropogenic layer (*unit I*) in various thicknesses, varying from 1.1 m in core E2 to 4.6 m in core E8 (Figure 5a, Figure 3). The sediments occur at depths between ~5.5 m and −2.5 m a.s.l., which means that in some cores they are even found up to 2 m above the floor level of the Temple of Bastet (i.e., in cores E1, E4, E5). Overall, the distribution of these fine-grained sediments (*unit II*) within the transect shows a basin-like shape in the southeast with the most clayey sediments in cores E5–E8 and maximum thicknesses and depths in cores E7 and E8. Ceramic fragments at the bottom of *unit II* in core E7 can be assigned to a period before the 25th dynasty (i.e., before c. 728 BCE). In core E5 an anthropogenic debris layer (*unit I*) separates two layers of fluvial/limnic deposits (*unit II*). In contrast, the anthropogenic debris layer in core E9 lies on top of the fluvial sands (*unit III*). Core E3, characterized only by an anthropogenic layer, was drilled to a maximum depth of four meters due to the presence of a solid layer that could not be breached.

In transect F, loamy to clayey deposits of fluvial/limnic origin (*unit II*) could only be found in core F2, which reached a thickness of 3.9 m and ranged from 0.5 m to −3.5 m a.s.l. The cores F1, F3, and F4 only show anthropogenic debris layers (*unit I*) on top of fluvial sands (*unit III*).

4.2. Electrical Resistivity Ranges and Distributions

The results of the ERT measurements are displayed together with the locations of the core sites and the simplified core stratigraphies in Figure 6. Overall, the geophysical and stratigraphical data show that the different lithological units of the study area can be roughly assigned to different resistivity ranges. While the clayey/loamy sediments of fluvial/limnic origin (*unit II*) can be associated with low resistivity values <50 Ωm, fluvial sands (*unit III*) generally show electric resistivity values > 100 Ωm. Resistivity values from ~10 to 400 Ωm can be associated with the anthropogenic debris layer (*unit I*).

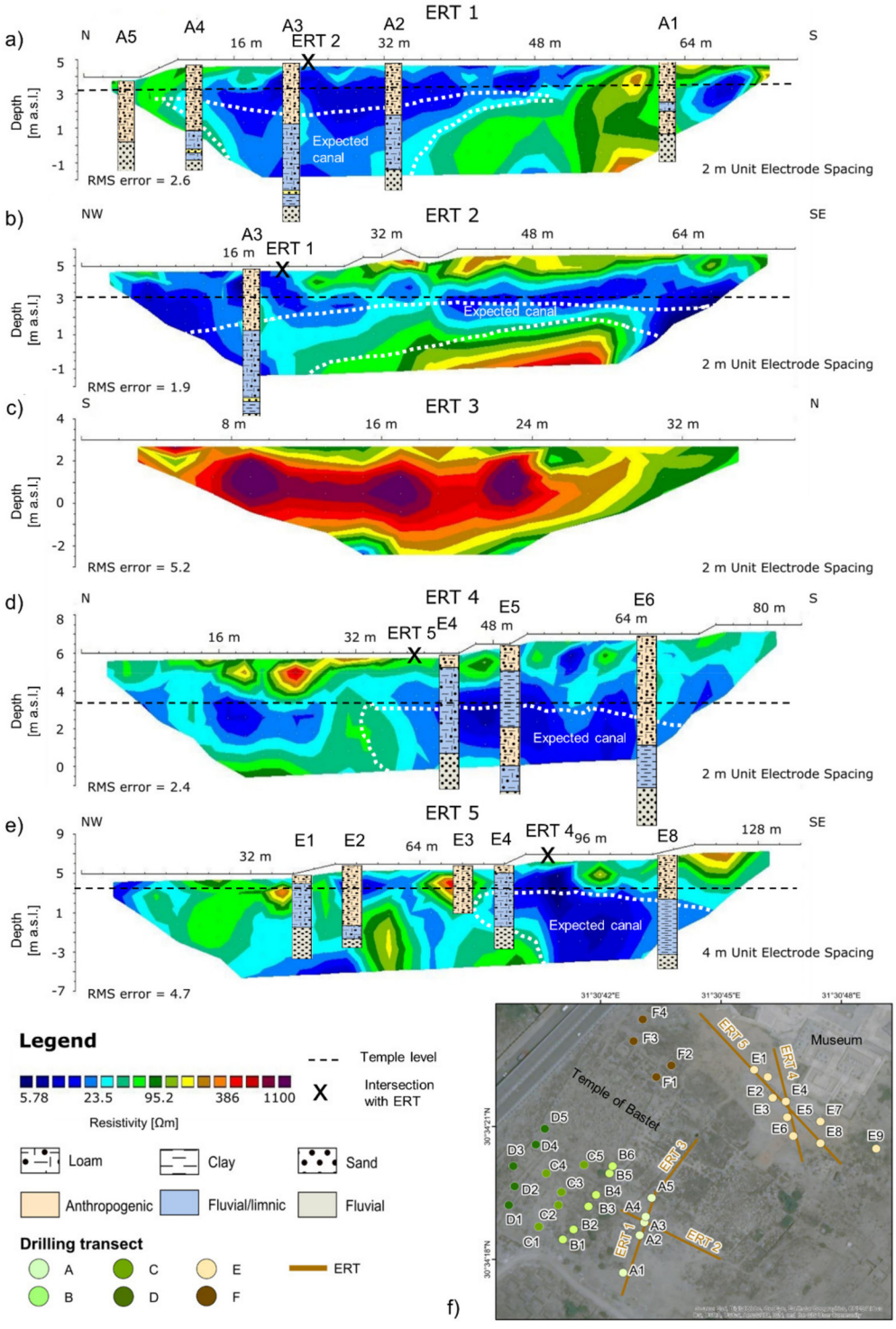

Figure 6. 2D Electrical Resistivity Tomography (ERT) profiles and drilling locations (**f**). The profiles ERT 1 and 2 are located south of the Temple of Bastet (**a**,**b**); profile ERT 3 is located in the center of the Temple of Bastet (**c**) and the profiles ERT 4 and 5 are located between the northern border of the Temple of Bastet and the museum (**d**,**e**). The dashed black line marks the ground level of the Temple of Bastet in the 1st millennium BCE (3.35 m a.s.l.). The dashed white line marks the extent of the expected canal.

4.2.1. South of the Temple of Bastet (Profiles ERT 1–2)

The profile ERT 1 extends from north to south and is located at the southern border of the Temple of Bastet (Figure 6a). Vertical resistivity changes divide the profile into three sections. The northern part displays resistivity values of approx. 25–100 Ωm, the southern part shows relatively high resistivity values up to 350 Ωm, interrupted by a zone of low resistivity values about 10 Ωm. The central section shows low resistivity values of about 10–30 Ωm at all depths. Combined with the stratigraphic information of cores A1 to A5, the higher resistivity values can be associated with the anthropogenic debris layer (*unit I*) and the *gezira* sands (*unit III*), while the lower ones are associated with loamy to clayey deposits of fluvial/limnic origin (*unit II*).

The profile ERT 2 extends from northwest to southeast and is located at the southern border of the Temple of Bastet (Figure 6b). Higher resistivity values (100–600 Ωm) of the basal layer indicate the occurrence of fluvial sands (*unit III*), while the medium-resistive subsurface layer (50–400 Ωm) is of varying size and most likely corresponds to the anthropogenic debris layer (*unit I*). The intermediate low-resistive layer (5–50 Ωm), which continues to spread into the western and eastern profile parts, can be associated with the loamy to clayey sediments of *unit II* as verified by core A3.

4.2.2. Center of the Temple of Bastet (Profile ERT 3)

The profile ERT 3 extends from south to north and is situated in the central part of the Temple of Bastet. Higher resistivity values from ~100–1100 Ωm indicate the occurrence of fluvial sands (*unit III*), as documented by former drillings in the temple area [2,13], and the presence of stone blocks representing remains of the temple (Figure 6c).

4.2.3. North of the Temple of Bastet (Profiles ERT 4–5)

The resistivity distributions north of the temple (ERT 4–5) are similar to those in the south (Figure 6d,e). The profile ERT 4 is located southwest of the museum and runs from north to south (Figure 6d). The depth profile can be divided into two parts. In the northern area, the uppermost subsurface layer reaches relatively high resistivity values of 70–400 Ωm, followed by lower resistivity values of around 10–100 Ωm. In the southern area, a 2–3 m thick subsurface layer shows resistivity values of up to 90 Ωm, followed by lower resistivity values of approx. 5–20 Ωm. The latter can be associated with clayey sediments of *unit II* as verified by cores E4, E5 and E6. The upper layer consists of anthropogenic debris (*unit I*).

The profile ERT 5 extends from northwest to southeast and is positioned southwest of the museum (Figure 6e). The depth profile can be divided into two parts. In the northern area, resistivity values of 50–400 Ωm occur, interspersed with isolated low resistivity areas <25 Ωm. In the southern area, a 2–3 m thick subsurface layer shows resistivity values of up to 300 Ωm, followed by significantly lower resistivity values of approx. 5–20 Ωm. The latter can be associated with loamy to clayey sediments of *unit II* as verified by cores E4 and E8. The layers of higher resistivity can often be associated with anthropogenic debris (*unit I*; cf. core E3 and E8).

5. Discussion

5.1. Sedimentary Units and ERT Surveying

The drilling campaigns in 2019 and 2020 revealed the occurrence of four different sedimentary units in the immediate vicinity of the temple, all of which differ in terms of their grain size compositions, color, moisture, and incorporation of anthropogenic artefacts. While the *units I–III* and their depositional milieus have been described and discussed in previous studies [2,13], *unit IV* is described here for the first time for Bubastis.

The light brownish to greyish sediments of the surface layer (*unit I*), composed of varying amounts of clay, silt, and fine sand, were predominantly formed by human activities [2], as evidenced by a large amount of anthropogenic remains such as pottery, brick, and limestone fragments, charcoal, and other finds such as plant remains and bones.

The loamy to clayey material of *unit II* together with its usually dark coloring suggest a high organic content and indicate the accumulation within a fluvial system of very low energy [59]. Comparable sediments have also been described as typical sediments of delta environments for other parts of the Nile Delta, e.g., for paleo-channels, ox-bow lakes and cut-offs [59–61]. In Bubastis these sediments most likely represent infills of former waterways or water bodies (i.e., canals; [2]). The varying amount of incorporated anthropogenic debris and the noticeable concentration of artefacts at the bottom of the lithological *unit II* in several cores indicate that these waterways were built and subsequently affected by human activity. This activity included anthropogenic backfilling and possible cleaning in order to allow the continuing performance of religious rites like the rowing of the sacred barque of Bastet.

The fluvial sands with varying gravel contents of *unit III* are most likely of Pleistocene age and can be addressed as *gezira* sands belonging to the *Geziracover Formation* [2,13,27,31], which is supported by the virtual absence of cultural debris within these deposits.

The sediments of *unit IV* can be interpreted as aeolian reworked *gezira* sands [31,62].

While the fluvial and aeolian sands of *units III* and *IV* can be easily distinguished from the other units, *units I* and *II* are somewhat more difficult to separate. Although the anthropogenic debris layer consists predominantly of silty to sandy sediments, it also contains fine-grained layers where the anthropogenic origin of the sediments is only indicated in conjunction with other sedimentological characteristics (i.e., artefact content, color, moisture). It should be noted that a possible misclassification of the depositional environment in individual cases cannot be excluded without further sedimentological and geochemical investigations.

ERT surveying was conducted in addition to the geomorphological investigations in order to extrapolate the results of sediment analyses to a larger area, i.e., to find evidence of the former course of the waterways. The results of the ERT surveying are generally in line with standard literature (e.g., [63,64]) and the observations from the sediment analyses. Thus, the coarser-grained anthropogenic debris layers (*unit I*: low soil moisture; varying grain sizes with high contents of silt and sand) of the upper one to six meters and the fluvial *gezira* sands (*unit III*: medium to coarse sand) underneath the Temple of Bastet and at the bottom of the profiles are usually characterized by higher resistivity values (>50 Ωm), whereas the loamy to clayey deposits of fluvial/limnic origin (*unit II*: loamy to clayey deposits; higher soil moisture) are characterized by lower resistivity values (<50 Ωm). The observed resistivity distributions are thus strongly influenced by stratigraphic differences in grain size [2].

However, the resistivity zones cannot always be clearly assigned to one lithostratigraphic unit, probably due to grain size variations and/or the influence of moisture and salinity [65,66]. For instance, the ERT measurements were not sensitive enough to discriminate the anthropogenic debris layers (*unit I*) from the underlying fluvial/limnic fine-grained deposits (*unit II*) consistently in all profiles. While in some profiles differentiation by resistivity values is consistent with the drilling results (e.g., for cores E4, E5, and E6 in ERT 4 and for core E8 in ERT 5), in other locations and profiles the anthropogenic debris layers are characterized by low resistivity values that are indistinguishable from those of the underlying fluvial/limnic sediments of *unit II* (e.g., in cores A2 and A3 in ERT 1 and A3 in ERT 2). The stratigraphic results of the cores therefore provide more reliable data on the distribution of anthropogenic debris in the study area. In contrast, the clayey deposits of fluvial/limnic origin (*unit II*) are essentially characterized by very low resistivity values, which is why they are used for the aerial detection of canal deposits below the temple level and in alignment with the drilling results in the profiles ERT 1, 2, 4, and 5 (see Figure 6).

Moreover, the presence of groundwater favors lower resistivity, as water has a higher electrical conductivity [63,64]. In the temple vicinity, the groundwater table lies at approx. −1.2 m a.s.l. [2], so it is likely that only profiles ERT 3 and ERT 5 are affected by groundwater, as indicated by the low resistivity at the bottom of the depth sections.

With the exception of the profile ERT 3 and ERT 2, *gezira* sands (*unit III*) are poorly depicted in the subsurface due to the shallow depths of the ERT sections and the decreasing horizontal resolution of ERT profiles with depth. The aeolian deposits of *unit IV* are too thin and not visible in the ERT depth profiles.

5.2. Canal Reconstruction

The fine-grained layers detected in the surroundings of the Temple of Bastet can be associated with the existence of a low energy fluvial system. The spatial distribution and thickness of these fine-grained sediments as observed in this study and in previous work [2], in conjunction with descriptions from historical texts, suggest the existence of a canal system that was connected to the Nile over an extended period of time.

Herodotus described two individual canals that were not connected. In addition to the detection of the northern canal in 2018 [2], the geomorphological and geophysical investigations south of the Temple of Bastet provide first evidence of the second canal. Fine-grained sediments detected in the drillings show a basin-like structure that most likely depicts a cross-section of an ancient canal that ran parallel to the temple (Figures 4 and 7). This is confirmed by the geoelectrical measurements, where profile ERT 1 shows a cross-section and profile ERT 2 a longitudinal section of the buried waterway (Figure 6a,b). Due to the occurrence and thickness of these loamy to clayey deposits, the center of the ancient canal can be assigned to cores A2 and A3 in transect A, cores B3 and B4 in transect B, and core C3 in transect C. Peripheral areas can be assigned to cores A1 and A2 in transect A, cores B2 and B5 in transect B, core C1 and C2 in transect C and core D1 in transect D. In total, the canal is 20 to 30 m wide, which confirms the description by Herodotus. The canal deposits occur at depths between ~3 m and −3.5 m a.s.l., placing them entirely below the floor level of the temple. At the deepest point in core A3, the canal bed is located about 6.8 m below temple level, which corresponds to the maximum canal depth in the area under investigation. The grain size distribution within these layers and transects ranges from loamy to clayey, indicating slightly different depositional conditions in the canal system, which could be due to different flow velocities and may have changed over time. Moreover, the alternation of anthropogenic and fluvial/limnic sediments in core C2 and the location of fine-grained sediments in cores B5 and C1 indicate anthropogenic sediment relocations. These could be the result of cleaning and maintenance activities as well as backfilling processes. Based on the drilling results and the geoelectrical survey, the course of the canal can be confirmed and traced over a length of about 150 m. This suggests that the canal ran relatively parallel to the temple, bending slightly in a southwesterly direction in the west (Figure 7).

In the area between the northern border of the Temple of Bastet and the site of the museum, fine-grained canal deposits were detected both in the drillings and in the geoelectrical measurements, supporting and extending the research results of previous investigations [2]. In the southeast, the center of a 30–35 m wide canal was detected in cores E5–E8 as indicated by thick layers of clayey deposits. Peripheral areas can be assigned to cores E1, E2, and E4 in transect E and F2 in transect F, characterized by coarser-grained loamy deposits. The ERT profiles ERT 1 and ERT 2 show cross sections of this buried waterway. The canal deposits occur at depths between ~5 m and −2.5 m a.s.l., indicating extensive sediment relocations, especially in the central to peripheral areas of the canal (cf. cores E4–E6), presumably due to cleaning and maintenance activities. At the deepest point in core E7, the canal bed lies about 5.8 m below the floor level of the temple. Based on the current results, the course of the canal cannot be completely reconstructed, but it can be assumed that similar to south of the temple, it ran relatively parallel to the temple, bending slightly in a northwesterly direction in the west.

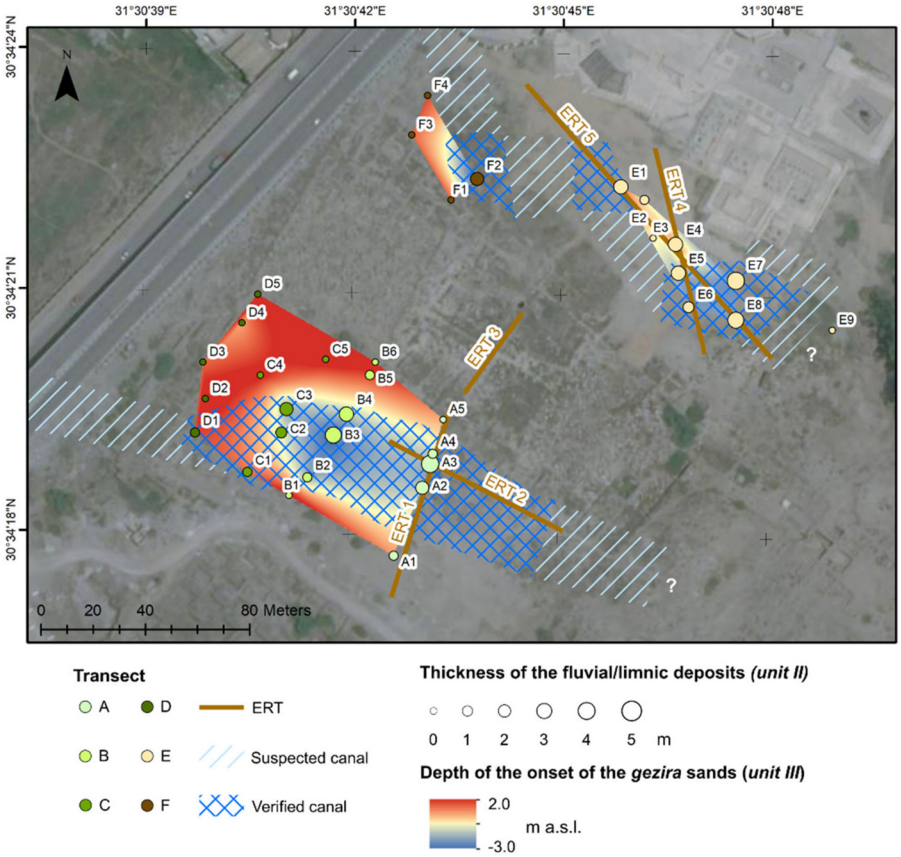

Figure 7. Depth of the onset of *gezira* sands (*unit III*), thicknesses of fluvial/limnic layers (*unit II*) and position of the verified/suspected canals (Database: © Esri Basemap).

Whether the occupants of Bubastis constructed these waterways or whether pre-existing natural channels were used and enhanced for this purpose cannot be conclusively determined. However, the immediate proximity to the temple and the verifiable parallel courses allude to the artificial construction of both canals. Ceramic fragments within the cores C2 and C3 in the southern canal date roughly in the period of the Old and Middle Kingdom (i.e., from c. 2700–1700 BCE), while pottery fragments at the canal base of core E7 in the northern canal date to a period before the 25th dynasty (i.e., before c. 728 BCE). This might indicate that the canals were already constructed in the early settlement and temple phases and were then in use for several centuries to millennia, although we cannot exclude the possibility that the material is intrusive, i.e., fell into the still existing canal at a later time, as the surface of the archaeological site is strewn with pottery. How long the canals were in use and at what time they were completely silted up, however, cannot be stated at present and must be clarified by further (geo)archaeological investigations.

Overall, it seems most likely that at least one feeder canal or natural channel existed which connected the temple canals with a main Nile branch. This also fits with Herodotus' description, which mentions that both canals were connected to the Nile but did not meet. Given the presumed location of the Pelusiac and Tanitic Nile branches (Figure 1b), it can be assumed that the canals were connected to the Nile in a westerly or northwesterly direction, probably also passing the Temple of Pepi I of the 6th dynasty (c. 2250 BCE; Figure 1c). However, this is a preliminary hypothesis that requires further investigation for verification. In addition, it must be clarified whether the canals ended in an easterly direction at the temple entrance or whether they possibly ran further through the city to the east (Figure 7).

6. Conclusions

The aim of this study was to localize the course of the sacred canals around the Temple of Bastet in the ancient city of Bubastis. In order to detect and obtain further detailed information about the course of these canals, 34 drillings as well as five 2D ERT surveys were conducted in 2019 and 2020, mainly at the northern and southern borders of the temple.

In the first few meters, mostly coarse-grained deposits of anthropogenic origin were detected, whereas the bottom layers of the cores are made of Pleistocene *gezira* sands typical for the region. In many cores, the anthropogenic debris layer is followed by fine-grained deposits of a dark color typical of increased organic content. These loamy to clayey deposits can be associated with a low-velocity fluvial system, proving the presence of two ancient canals in the direct vicinity of the Temple of Bastet. Beside the basin-like distribution of the canal sediments within the drilling transects, the course of the canals can be additionally reconstructed by the 2D ERT depth profiles. Accordingly, two separate and approx. 30 m wide canals can be located north and south of the Temple of Bastet with an approx. length of 150 m. The immediate proximity to the temple and the verifiable parallel courses allude to an artificial construction of both canals. In addition, the distribution of canal deposits and the incorporation of numerous artefacts indicate increased human activity, such as canal cleaning to allow for the continued performance of religious rites such as the rowing of the barque of Bastet. Ceramic fragments yielded dates from the Old Kingdom to the Third Intermediate Period of Egypt (c. 2700–700 BCE), suggesting that the canals were constructed relatively early and were in use for several centuries to millennia. However, it remains to be clarified when exactly the canals were built and how long they were in use.

From an Egyptological and geoarchaeological point of view, the results of the study are most remarkable as for the first time they provide geoarchaeological proof of the existence of sacred water bodies, i.e., the most important elements of the sacred landscape of temples in the Nile Delta. This is particularly striking, as our knowledge was hitherto limited to descriptions from ancient literary sources of limited reliability. Now, based on new geophysical and sedimentological analyses, the course and width of the canals described by Herodotus could be verified in the southern and northern surroundings of the Temple of Bastet in ancient Bubastis. Most likely, these waterways were connected to the Nile in a westerly or northwesterly direction. However, the areas to the east and west of the temple need further geoarchaeological investigation to fully reconstruct the temple's sacred waterscape and to determine how the canals were connected to the Nile and whether they flowed through the residential city.

Supplementary Materials: The following are available online at https://www.mdpi.com/article/10.3390/geosciences11090385/s1, Table S1: Detailed descriptions of the core profiles from the surroundings of the Temple of Bastet in ancient Bubastis.

Author Contributions: Conceptualization, J.M., J.T., E.L.-A. and A.A.E.-R.; Data curation, J.M. and A.A.E.-R.; Formal analysis, J.M., P.G., J.T., A.E.-S. and A.A.E.-R.; Funding acquisition, T.U. and E.L.-A.; Investigation, J.M., P.G., J.T. and A.A.E.-R.; Methodology, J.M., J.T. and A.A.E.-R.; Project administration, J.M.; Resources, J.M., R.B. and E.L.-A.; Software, P.G., J.T. and A.A.E.-R.; Supervision, J.M. and E.L.-A.; Validation, J.M., P.G., J.T. and A.A.E.-R.; Visualization, J.M., P.G., J.T., T.U. and A.A.E.-R.; Writing—original draft, J.M., P.G., E.L.-A. and A.A.E.-R.; Writing—review & editing, J.M., P.G., J.T., T.U., A.E.-S., R.B., E.L.-A. and A.A.E.-R. All authors have read and agreed to the published version of the manuscript.

Funding: This research has been funded by the research fund of the Faculty of Philosophy of the University of Würzburg (Die Sakrallandschaft von Bubastis: Geoarchäologische Untersuchungen zu den heiligen Wasserkanälen des Tempels der Bastet).

Data Availability Statement: The datasets generated during and/or analyzed during the current study are available from the corresponding author on reasonable request.

Acknowledgments: We thank the German Archaeological Institute Cairo and the project group around Jürgen Wunderlich (University of Frankfurt) and Robert Schiestl (University of Munich) for the use of their drilling equipment. The Digital Elevation Model of the TanDEM-X Mission is shown with the permission of the German Aerospace Center (DLR); related proposal: "DEM_HYDR1426 - Geoarchaeology of the Nile Delta, an integrated research collaboration of the University of Würzburg and University of Frankfurt that seeks to deduce geomorphological and palaeoenvironmental information from Tandem-X DEM data"; Principal Investigators: A. Ginau, R. Schiestl, J. Wunderlich, E. Lange-Athinodorou, T. Ullmann. We acknowledge the use of imagery from the Worldview Snapshots application (https://wvs.earthdata.nasa.gov/), part of the Earth Observing System Data and Information System (EOSDIS). We also thank Katharine Thomas for proofreading the manuscript.

Conflicts of Interest: The authors declare no conflict of interest. The funders had no role in the design of the study; in the collection, analyses or interpretation of data; in the writing of the manuscript, or in the decision to publish the results.

References

1. Bussmann, R. Die Provinztempel Ägyptens Von der 0. Bis Zur 11. Dynastie. In *Probleme der Ägyptologie*; Brill: Leiden, The Netherlands, 2010; ISBN 978-90-04-17933-2.
2. Lange-Athinodorou, E.; El-Raouf, A.A.; Ullmann, T.; Trappe, J.; Meister, J.; Baumhauer, R. The sacred canals of the Temple of Bastet at Bubastis (Egypt): New findings from geomorphological investigations and Electrical Resistivity Tomography (ERT). *J. Archaeol. Sci. Rep.* **2019**, *26*, 101910. [CrossRef]
3. Lange-Athinodorou, E. Implications of geoarchaeological investigations for the contextualization of sacred landscapes in the Nile Delta. *EG Quat. Sci. J.* **2021**, *70*, 73–82. [CrossRef]
4. Gessler-Löhr, B. Die Heiligen Seen Ägyptischer Tempel: Ein Beitrag Zur Deutung Sakraler Baukunst im Alten Ägypten. In *Hildesheimer Ägyptologische Beiträge*; Gerstenberg: Hildesheim, Germany, 1983; Volume 21, ISBN 978-3-8067-8080-2.
5. Richter, B.A. On the Heels of the Wandering Goddess: The Myth and the Festival at the Temples of the Wadi el-Hallel and Dendera. In *8. Ägyptologische Tempeltagung: Interconnections between Temples*; Dolińska, M., Beinlich, H., Eds.; Harrassowitz Verlag: Wiesbaden, Germany, 2010.
6. Tillier, A. Notes sur l'icherou. *Égypte Nilotique Mediterr.* **2010**, *3*, 167–176.
7. Trampier, J. Reconstructing the Desert and Sown Landscape of Abydos. *J. Am. Res. Cent. Egypt.* **2005**, *42*, 73–80.
8. Atya, M.A.; Al Khateeb, S.O.; Ahmed, S.B.; Musa, M.F.; Gaballa, M.; Abbas, A.M.; Shaaban, F.F.; Hafez, M.A. GPR investigation to allocate the archaeological remains in Mut temple, Luxor, Upper Egypt. *NRIAG J. Astron. Geophys.* **2012**, *1*, 12–22. [CrossRef]
9. Wilson, P. The survey of Saïs (Sa el-Hagar) 1997–2002. In *Egypt Exploration Society, Excavation Memoir*; Egypt Exploration Society: London, UK, 2006; ISBN 978-0-85698-175-3.
10. Wilson, P. Gateway to the underworld: The cult areas at Sais. *Stud. Anc. Egypt. Sudan* **2019**, *24*, 341–364.
11. Leclère, F. *Les Villes de Basse Égypte au Ier Millénaire av. J.-C.: Analyse Archéologique et Historique de la Topographie Urbaine*; Bibliothèque d'étude; Institut Français D'archéologie Orientale: Cairo, Egypt, 2008; Vol. 2, ISBN 978-2-7247-0489-1.
12. Montet, P. Le lac sacré de Tanis. In *Académie des Inscriptions et Belles-Lettres (Extrait des Mémoires de l'Académie, Tome XLIV)*; Imprimerie Nationale: Paris, France, 1966.
13. Ullmann, T.; Lange-Athinodorou, E.; Göbel, A.; Büdel, C.; Baumhauer, R. Preliminary results on the paleo-landscape of Tell Basta/Bubastis (eastern Nile delta): An integrated approach combining GIS-Based spatial analysis, geophysical and archaeological investigations. *Quat. Int.* **2019**, *511*, 185–199. [CrossRef]
14. Maillet, G.M.; Rizzo, E.; Revil, A.; Vella, C. High Resolution Electrical Resistivity Tomography (ERT) in a Transition Zone Environment: Application for Detailed Internal Architecture and Infilling Processes Study of a Rhône River Paleo-channel. *Mar. Geophys. Res.* **2005**, *26*, 317–328. [CrossRef]
15. Rowland, J.; Strutt, K.D. Geophysical survey and sub-surface investigations at Quesna and Kom el-Ahmar (Minuf), governorate of Minufiyeh: An integrated strategy for mapping and understanding sub-surface remains of mortuary, sacred and domestic contexts. In Proceedings of the International Conference "Achievements and Problems of Modern Egyptology", Moscow, Russia, 29 September–2 October 2009; Belova, G.A., Ivanov, S.V., Eds.; Russian Academy of Sicences, Center for Egyptological Studies: Moscow, Russia, 2012; pp. 328–345.
16. Torrese, P.; Rainone, M.L.; Colantonio, F.; Signanini, P. Identification and investigation of shallow paleochannels in the chamelecon valley (Honduras): 1D vs. 2D electrical resistivity surveys. In *Symposium on the Application of Geophysics to Engineering and Environmental Problems 2013*; Environmental and Engineering Geophysical Society: Denver, CO, USA, 2013; pp. 321–331.
17. El-Kenawy, A.; Metwaly, M.; Gemail, K.; El-Raouf, A.A. Contribution of geoelectrical resistivity sounding for paleoenvironment assessment at Saft El-Henna and Tell El-Dab'a archaeological sites, eastern Nile Delta, Egypt. *Explor. Geophys.* **2013**, *44*, 282–288. [CrossRef]
18. Kasprzak, M.; Traczyk, A. LiDAR and 2D Electrical Resistivity Tomography as a Supplement of Geomorphological Investigations in Urban Areas: A Case Study from the City of Wrocław (SW Poland). *Pure Appl. Geophys.* **2014**, *171*, 835–855. [CrossRef]

19. El-Gamili, M.M.; Shaaban, F.F.; El-Morsi, O.A. Electrical resistivity mapping of the buried stream channel of the Canopic branch in the western Nile Delta, Egypt. *J. Afr. Earth Sci.* **1994**, *19*, 135–148. [CrossRef]
20. El Gamili, M.M.; Ibrahim, E.H.; Hassaneen, A.R.G.; Abdalla, M.A.; Ismael, A.M. Defunct Nile Branches Inferred from a Geoelectric Resistivity Survey on Samannud area, Nile Delta, Egypt. *J. Archaeol. Sci.* **2001**, *28*, 1339–1348. [CrossRef]
21. Toonen, W.H.J.; Graham, A.; Pennington, B.T.; Hunter, M.A.; Strutt, K.D.; Barker, D.S.; Masson-Berghoff, A.; Emery, V.L. Holocene fluvial history of the Nile's west bank at ancient Thebes, Luxor, Egypt, and its relation with cultural dynamics and basin-wide hydroclimatic variability. *Geoarchaeology* **2018**, *33*, 273–290. [CrossRef]
22. Altmeyer, M.; Seeliger, M.; Ginau, A.; Schiestl, R.; Wunderlich, J. Reconstruction of former channel systems in the northwestern Nile Delta (Egypt) based on corings and electrical resistivity tomography (ERT). *EG Quat. Sci. J.* **2021**, *70*, 151–164. [CrossRef]
23. Wilson, P.; Ghazala, H. Sandhills, sandbanks, waterways, canals and sacred lakes at Sais in the Nile Delta. *EG Quat. Sci. J.* **2021**, *70*, 129–143. [CrossRef]
24. Shata, A.A.; El Fayoumy, I.F. Remarks on the regional geological structure of the Nile Delta. In Proceedings of the Bucharest Symposium on Hydrogeology of Deltas, Bucharest, Romania, 6–14 May 1969; Gentbrugge Belgium: Paris, France, 1970; pp. 189–197.
25. Butzer, K.W. *Early Hydraulic Civilization in Egypt: A Study in Cultural Ecology*; University of Chicago Press: Chicago, IL, USA, 1976; ISBN 978-0-226-08635-4.
26. Said, R. *The Geological Evolution of the River Nile*; Springer: New York, NY, USA, 1981; ISBN 978-1-4612-5843-8.
27. Andres, W.; Wunderlich, J. Late Pleistocene and Holocene Evolution of the Eastern Nile Delta and Comparisons with the Western Delta. In *Von der Nordsee bis Zum Indischen Ozean. Ergebnisse der 8. Jahrestagung des AK Geographie der Meere und Küsten*; Brückner, H., Ratdke, U., Eds.; Erdkundliches Wissen: Stuttgart, Germany, 1991; pp. 121–130.
28. Stanley, D.J.; Warne, A.G. Nile Delta in Its Destruction Phase. *J. Coast. Res.* **1998**, *14*, 795–825.
29. Stanley, D.J.; Warne, A.G. Nile Delta: Recent Geological Evolution and Human Impact. *Science* **1993**, *260*, 628–634. [CrossRef]
30. Goodfriend, G.A.; Stanley, D.J. Rapid strand-plain accretion in the northeastern Nile Delta in the 9th century A.D. and the demise of the port of Pelusium. *Geology* **1999**, *27*, 147–150. [CrossRef]
31. Pennington, B.T.; Sturt, F.; Wilson, P.; Rowland, J.; Brown, A.G. The fluvial evolution of the Holocene Nila. *Quat. Sci. Rev.* **2017**, *170*, 212–231. [CrossRef]
32. Butzer, K.W. Geoarchaeological implications of recent research in the Nile Delta. In *Egypt and the Levant: Interrelations from the 4th through the Early 3rd Millennium BCE*; van den Brink, E.C.M., Levy, T.E., Eds.; Leicester University Press: London, UK; New York, NY, USA, 2002; pp. 83–97.
33. Meister, J.; Lange-Athinodorou, E.; Ullmann, T. Preface: Special issue "Geoarchaeology of the Nile Delta". *EG Quat. Sci. J.* **2021**, *70*, 187–190. [CrossRef]
34. Van den Brink, E.C.M. A geo-archaeological survey in the north-eastern Nile Delta. *Mitt. Dtsch. Archäol. Inst. Abt. Kairo* **1986**, *43*, 7–31.
35. Said, R. *The River Nile: Geology, Hydrology and Utilization*; Pergamon Press: Oxford, UK; New York, NY, USA; Seoul, Korea; Tokyo, Japan, 1993; ISBN 978-0-08-041886-5.
36. Bietak, M. Tell El-Dab'a II, Der Fundort im Rahmen Einer Archäologisch-Geographischen Untersuchung Über das Ägyptische Ostdelta. In *Untersuchungen der Zweigstelle Kairo des Österreichischen Archäologischen Instituts*; Verlag der Österreichischen Akademie der Wissenaschaften: Wien, Austria, 1975; ISBN 978-0-00-343931-1.
37. El Mahmoudi, A.; Gabr, A. Geophysical surveys to investigate the relation between the Quaternary Nile channels and the Messinian Nile canyon at East Nile Delta, Egypt. *Arab. J. Geosci.* **2009**, *2*, 53–67. [CrossRef]
38. Ullmann, T.; Nill, L.; Schiestl, R.; Trappe, J.; Lange-Athinodorou, E.; Baumhauer, R.; Meister, J. Mapping buried paleogeographical features of the Nile Delta (Egypt) using the Landsat archive. *EG Quat. Sci. J.* **2020**, *69*, 225–245. [CrossRef]
39. Lange, E. Die Ka-Anlage Pepis I. in Bubastis im Kontext königlicher Ka-Anlagen des alten Reiches. *Z. Ägypt. Sprache Altert.* **2006**, *133*, 121–140. [CrossRef]
40. Bakr, M.I.; Lange, E. Die Nekropolen des Alten Reichs in Bubastis. In *Ägypten Begreifen. Erika Endesfelder in Memoriam*; Feder, F., Sperveslage, G., Steinborn, F., Eds.; IBAES 19: Berlin, Germany; London, UK, 2017; pp. 31–48.
41. Lange-Athinodorou, E.; Es-Senussi, A. A royal ka-temple and the rise of Old Kingdom Bubastis. *Egypt. Archaeol.* **2021**, *53*, 20–24.
42. Bietak, M.; Lange, E. Tell Basta: The palace of the Middle Kingdom. *Egypt. Archaeol.* **2014**, *44*, 4–7.
43. Lange, E. The So-called Governors' Cemetery at Bubastis and Provincial Elite. Tombs in the Nile Delta: State and Perspectives of Research. In *The World of Middle Kingdom Egypt (2000–1550 BC)*; Grajetzki, M., Ed.; GHP Egyptology: London, UK, 2015.
44. Lange, E.; Ullmann, T.; Baumhauer, R. Remote Sensing in the Nile Delta: Spatio-Temporal Analysis of Bubastis/Tell Basta. *Ägypt. Levante/Egypt Levant* **2016**, *26*, 377–392. [CrossRef]
45. Lange, E. Legitimation und Herrschaft in der Libyerzeit. Eine neue Inschrift Osorkons I. aus Bubastis (Tell Basta). *Z. Ägypt. Sprache Kult* **2008**, *135*, 131–141. [CrossRef]
46. Lange, E. The Sed-festival of Osorkon II. at Bubastis: New investigations. In *The Libyan Period in Egypt. Historical and Cultural Studies into the 21st–24th Dynasties: Proceedings of a Conference at Leiden University, 25–27 October 2007*; Broekman, G.P.F., Demare, R.J., Kaper, O., Eds.; Nederlands Instituut voor het Nabije Osten: Leiden, The Netherlands, 2009.
47. Lange-Athinodorou, E. Der "Tempel des Hermes" und die Pfeile der Bastet: Zur Rekonstruktion der Kulturlandschaft von Bubastis. In *Festschrift Hans-Werner Fischer-Elfert*; De Gruyter: Berlin, Germany, 2019; pp. 549–585.

48. Lange-Athinodorou, E. Sedfestritual und Königtum: Die Reliefdekoration am Torbau Osorkons II. im Tempel der Bastet von Bubastis. In *Ägyptologische Abhandlungen*; Harrassowitz: Wiesbaden, Germany, 2019; ISBN 978-3-447-11192-8.
49. Kitchen, K.A. *The Third Intermediate Period in Egypt (1100-650 BC)*; Aris & Philipps: Warminster, UK, 1986; ISBN 978-0-85668-298-8.
50. Naville, E. Bubastis (1887–1889). In *Memoir of the Egypt Exploration Fund*; Kegan Paul, Trench, Truebner: London, UK, 1891.
51. Meeks, D. Mythes et légendes du Delta d'après le papyrus Brooklyn 47.218.84. In *Mémoires Publiés par les Membres de l'Institut Français d'Archéologie Orientale*; Institut Français d'Archéologie Orientale: Cairo, Egypt, 2006; ISBN 978-2-7247-0427-3.
52. Wilson, N.G. *Herodoti Historiae*; Oxford University Press: Oxford, UK, 2015; ISBN 978-0-19-956071-4.
53. Ullmann, T.; Büdel, C.; Brauneck, J.; Lange, E.; Baumhauer, R. Landoberflächenanalyse zur Identifikation antiker Wasserwege im Umfeld der Tempelanlagen von Bubastis im südöstlichen Nildelta. *DGPF Tag.* **2015**, *24*, 280–287.
54. Ad-hoc-Arbeitsgruppe Boden. *Bodenkundliche Kartieranleitung. KA5 [Manual of Soil Mapping]*, 5th ed.; Eckelmann, W., Ed.; Schweizerbart Science Publishers: Stuttgart, Germany, 2005; ISBN 978-3-510-95920-4.
55. FAO. *World Reference Base for Soil Resources 2014. International Soil Classification System for Naming Soils and Creating Legends for Soil Maps–Update 2015*; World Soil Resources Reports; Food and Agriculture Organization of the United Nations: Rome, Italy, 2015; ISBN 978-92-5-108369-7.
56. Dahlin, T.; Zhou, B. A numerical comparison of 2D resistivity imaging with 10 electrode arrays. *Geophys. Prospect.* **2004**, *52*, 379–398. [CrossRef]
57. Papadopoulos, N.G.; Tsourlos, P.; Tsokas, G.N.; Sarris, A. Two-dimensional and three-dimensional resistivity imaging in archaeological site investigation. *Archaeol. Prospect.* **2006**, *13*, 163–181. [CrossRef]
58. Loke, M.H.; Barker, R.D. Rapid least-squares inversion of apparent resistivity pseudosections by a quasi-Newton method1. *Geophys. Prospect.* **1996**, *44*, 131–152. [CrossRef]
59. Ginau, A.; Schiestl, R.; Wunderlich, J. Integrative geoarchaeological research on settlement patterns in the dynamic landscape of the northwestern Nile delta. *Quat. Int.* **2019**, *511*, 51–67. [CrossRef]
60. Brown, A.G. Alluvial Geoarchaeology: Floodplain Archaeology and Environmental Change. In *Cambridge Manuals in Archaeology*; Cambridge University Press: Cambridge, UK; New York, NY, USA, 1997; ISBN 978-0-521-56097-9.
61. Toonen, W.H.J.; Kleinhans, M.G.; Cohen, K.M. Sedimentary architecture of abandoned channel fills. *Earth Surf. Process. Landf.* **2012**, *37*, 459–472. [CrossRef]
62. Wunderlich, J. Investigations on the development of the Western Nile Delta in Holocene times. In *The Archaeology of the Nile Delta, Egypt: Problems and Priorities: Proceedings of the Seminar Held in Cairo, 19–22 October 1986*; van den Brink, E.C.M., Ed.; Netherlands Foundation for Archaeological Research in Egypt: Amsterdam, The Netherlands, 1988; pp. 251–257.
63. Telford, W.M.; Geldart, L.P.; Sheriff, R.E. *Applied Geophysics*, 2nd ed.; Cambridge University Press: Cambridge, UK, 1990; ISBN 978-0-521-32693-3.
64. Reynolds, J.M. *An Introduction to Applied and Environmental Geophysics*, 2nd ed.; Wiley: Hoboken, NJ, USA, 2011; ISBN 978-0-471-48535-3.
65. Choudhury, K.; Saha, D.K.; Chakraborty, P. Geophysical study for saline water intrusion in a coastal alluvial terrain. *J. Appl. Geophys.* **2001**, *46*, 189–200. [CrossRef]
66. Shaaban, F.F.; Shaaban, F.A. Use of two-dimensional electric resistivity and ground penetrating radar for archaeological prospecting at the ancient capital of Egypt. *J. Afr. Earth Sci.* **2001**, *33*, 661–671. [CrossRef]